

**Solid state structural relation and binary melting phase diagram of (*S*-) and racemic  
2-(2-nitro-1-phenylethyl)-1,3-diphenyl-propane-1,3-dione.**

Katalin Gönczi<sup>a</sup>, Veronika Kudar<sup>b</sup>, Zsuzsa Jászay<sup>c</sup>, Petra Bombicz<sup>b</sup>, Ferenc Faigl<sup>a,c</sup>, János Madarász<sup>d,\*</sup>

<sup>a</sup>Department of Organic Chemistry and Technology, Budapest University of Technology and Economics, H-1521 Budapest, Hungary. <sup>b</sup>Institute of Organic Chemistry, Research Centre for Natural Sciences, Hungarian Academy of Sciences, 1525 Budapest, Hungary.

<sup>c</sup>MTA-BME Organic Chemical Technology Research Group, Hungarian Academy of Sciences, 1521 Budapest, Hungary. <sup>d</sup>Department of Inorganic and Analytical Chemistry, Budapest University of Technology and Economics, H-1521 Budapest, Hungary

### **Abstract**

Both enantiomeric (*S*-) and racemic (*RS*-) forms of 2-(2-nitro-1-phenylethyl)-1,3-diphenyl-propane-1,3-dione (**1**) have been obtained from the same reaction media by fractional crystallization from toluene. First the racemic compound, (*R,S*)-**1** has been precipitated (mp. 159.7°C), then, from the filtrate, its chiral form, (*S*)-**1** (mp. 135.6°C) has crystallized. The absolute molecular configuration (*S*) and crystal structure of the latter one, which crystallizes in the orthorhombic crystal system (space group  $P2_12_12_1$  (19),  $a = 10.6377(2)$  Å,  $b = 11.4348(2)$  Å,  $c = 31.3543(6)$  Å,  $Z = 8$ ,  $Z' = 2$ ), has been solved by single crystal X-ray diffraction ( $R = 0.0377$ ). Powder XRD pattern of the racemic precipitation, (*R,S*)-**1** could be indexed in the orthorhombic space group  $Pbca$  (61) ( $a = 22.18(7)$  Å,  $b = 17.08(3)$  Å,  $c = 9.96(3)$  Å,  $Z = 8$ ,  $Z' = 1$ ). Differences in the secondary bonding interactions and in crystal stability of the chiral and racemic compound are evaluated on the basis of their FT-IR spectrum, melting point and enthalpy of fusion. The eutectic type binary melting phase diagram of enantiomeric and racemic compounds are constructed based on the Differential Scanning Calorimetric (DSC) measurements and calculation of the liquidus curves according to the combination of the simplified Schröder-van Laar and Prigogine-Defay equations.

### **Keywords**

Enantioselective Michael addition, dibenzoylmethane, *trans*-2-nitrostyrene, single crystal and powder X-ray diffraction (XRD), crystal structure determination, FT-IR spectroscopy, Differential Scanning Calorimetry (DSC), binary melting phase diagrams, eutectic compositions and temperatures, structure-property relationship

---

\* Corresponding author. Fax: +36-1-463-3408; e-mail: [madarasz@mail.bme.hu](mailto:madarasz@mail.bme.hu) (J. Madarász)

## 1. Introduction

Optically active nitroalkanes, among them 2-(2-nitro-1-phenylethyl)-1,3-diphenyl-propane-1,3-dione (*S*)-**1** [<sup>1,2,3</sup>] are versatile building blocks in organic synthesis as they can be transformed into various chiral amines, oxo compounds, carboxylic acids, etc. The most common way of its synthesis is the asymmetric Michael addition of 1,3-diphenyl-propane-2,5-dion (**2**) to a *trans*- $\beta$ -nitrostyrene (**3**) in the presence of a chiral catalyst (Scheme 1).

### **Scheme 1: Regio and enantioselective synthesis of the title compounds**

Application of various chiral catalysts also resulted in preparation of enantiomeric forms of several derivative or related compounds, in reasonable optical purity and product yield. [<sup>4,5,6,7,8,9</sup>]. Most of the major optically active products are assigned as (*S*)-configuration based on various predictions and on the solved structure of a chloro substituted derivative of (**1**)[2].

However, in most cases the optical purity of the enantiomerically enriched products needs further improvement. While resolution via diastereomeric salt or derivative formation is dominant in separation of optical isomers, in some cases fractional crystallization can be a simple, alternative possibility. The advantage of the latter, that no chiral additive is needed. In this paper we report a successful route of enantiomeric enrichment of 2-(2-nitro-1-phenylethyl)-1,3-diphenyl-propane-1,3-dione (**1**) via fractional crystallization.

Thereafter, having both racemic and enantiomeric 2-(2-nitro-1-phenylethyl)-1,3-diphenyl-propane-1,3-dione in hand, we have carried out a comparative study on the secondary bonding interactions of their structures effecting their mixing properties in solutions and solid phase, i.e. their solubility and melting behavior. Absolute molecular configuration and crystal structure of the enantiomeric crystal, (*S*)-**1** has been solved by single crystal X-ray diffraction, while powder pattern of the precipitated racemic compound, (*R,S*)-**1** has also been indexed. The effect of structural differences between

the pure enantiomer and the racemic crystals has also been evaluated on the basis of their Fourier transform infrared spectra and differential scanning calorimetric (DSC) curves. Based on DSC measurements of temperature of fusion and melting molar enthalphy, together with DSC observations also for some physical mixtures of (*S*)-**1** and (*R,S*)-**1**, liquidus curves, eutectic temperature and composition have been calculated; in overall, a schematic binary phase diagram has been constructed.

## 2. Experimental

### 2.1. Starting materials and sample preparations

1,3-diphenyl-1,3-propanedione (98%, Aldrich D33454), *trans*- $\beta$ -nitrostyrene (99%, Aldrich N26806) and quinidine (Aldrich Q3625) were purchased from Sigma-Aldrich. Dichloromethane (Merck 8.22271), toluene (Merck 1.08323) and triethylamine (Merck 8.08352) were purchased from Merck. Chemicals were used without further purification.

Synthesis of (*RS*)-2-(2-nitro-1-phenylethyl)-1,3-diphenyl-propane-1,3-dione (*R,S*)-**1**: To a solution of 0.2 mmol (0.03 g) *trans*- $\beta$ -nitrostyrene **3** and 0.2 mmol (0.02 g) triethylamine (**4a**) in dichloromethane (4 ml) 1,3-diphenyl-1,3-propanedione **2** (0.22 mmol, 0.05 g) dissolved also in dichloromethane (2ml) was added. The reaction mixture was stirred at room temperature and monitored by TLC. The solvent was evaporated and the residue was purified by column chromatography on silica gel using hexane-ethyl acetate = 7:3 as an eluent resulting in a white solid (0.058 g, yield: 78%).

For enantioselective preparation of (*S*)-**1** the same procedure was followed, except that instead of triethylamine a chiral catalyst, quinidine (**4b**, 0.02 mmol) was used. After column chromatography 0.55 g (74%) (*S*)-**1** (*ee*:42%) white solid was obtained. The catalyst was also recovered during column chromatography.

<sup>1</sup>H-NMR (500 MHz, CDCl<sub>3</sub>):  $\delta$  (ppm): 4.64 (1H, dd, *J* = 7.5, 14.3 Hz, Ph-CH); 5.01-5.15 (2H, m, CH<sub>2</sub>NO<sub>2</sub>); 5.85 (1H, d, *J* = 8.0); 7.18-7.34 (15H, m, Ar).

<sup>13</sup>C-NMR (300 MHz, CDCl<sub>3</sub>):  $\delta$  (ppm): 43.4; 59.5; 76.8; 127.5; 127.7; 128.2; 128.9; 129.52; 133.7; 134.2; 135.6; 136.2; 136.8; 195.2; 196.6.

HPLC conditions: Chiraldpak AS-H (hexane-IPA:85:15, flow rate 1 ml/min, 210 nm, 10 °C)  $t_{\text{major}}=19.3$  min and  $t_{\text{minor}}=38.8$  min.

Fractional crystallization: 0.2 g of (*S*)-**1** (*ee*: 42%) product was recrystallized twice from 2 ml of toluene. The mixture was kept on 5°C for 2 hrs before crystallization. The results are summarized in Table 1.

Table 1. Crystallization process of the products from enantioselective synthesis for (*S*)-**1**.

Compound to be crystallized	Precipitate filtered from toluene solution			Crystals from the filtrate		
	$[\alpha]_D^{20}$ (C=1) CHCl <sub>3</sub>	<i>ee</i> (%) <sup>a</sup>	Yield (%)	$[\alpha]_D^{20}$ (C=1) CHCl <sub>3</sub>	<i>ee</i> (%) <sup>a</sup>	Yield (%)
( <i>S</i> )- <b>1</b> ( <i>ee</i> :42%)  (obtained by synthesis)	-	0	54	20.6	94	46
( <i>S</i> )- <b>1</b> ( <i>ee</i> :94%)  (obtained by fract.crystallization)	21.0	96	53	20.2	93	44

<sup>a</sup>*ee* values were determined by HPLC using a chiral column,

Single crystal growth. The white single crystals of the (*S*)-2-(2-nitro-1-phenylethyl)-1,3-diphenyl-propane-1,3-dione (*S*)-**1** were grown in abs. ethanol.

The binary mixtures of enantiomeric and racemic compounds for DSC trials, were prepared from the solids by appropriate weighting and gentle grounding together to achieve 50 and 82% enantiomeric excess of (*S*)-enantiomer ( $x_s = 0.75$  and  $x_s = 0.91$ , respectively).

## 2.2. Single crystal X-ray diffraction

A colourless, block crystal of  $C_{23}H_{19}NO_4$  having approximate dimensions of  $0.77 \times 0.42 \times 0.41$  mm was mounted on a loop. All measurements were made on a Rigaku R-Axis RAPID imaging plate area detector diffractometer with graphite monochromated Cu-K $\alpha$  radiation ( $\lambda = 1.54187$  Å) at  $93(2)$  K in the range of  $6.85 \leq \theta \leq 71.74^\circ$ . Cell parameters were determined by least-squares of the setting angles of 9499 ( $6.85 \leq \theta \leq 71.21^\circ$ ) reflections. A total 46848 reflections were collected [<sup>10</sup>] of which 6957 were unique ( $R_{int} = 0.0328$ ); intensities of 6494 reflections were greater than  $2\sigma(I)$ . Completeness to  $\theta = 0.960$ . For  $Z = 8$  and F.W. = 373.39, the calculated density is  $1.301$  g/cm $^3$ . The systematic absences uniquely determine the space group to be:  $P\bar{2}_12_12_1$  (s.g. No. 19). A numerical absorption correction [<sup>11</sup>] was applied which resulted in transmission factors ranging from 0.843 to 0.676. The linear absorption coefficient,  $\mu$ , for **1** with Cu-K $\alpha$  radiation is  $0.728$  mm $^{-1}$ .

The structure was solved by direct methods [<sup>12</sup>]. Anisotropic full-matrix least-squares refinement [12] on  $F^2$  for all non-hydrogen atoms yielded  $R_I = 0.0377$  and  $wR^2 = 0.0859$  for 6494 [ $I > 2\sigma(I)$ ] and  $R_I = 0.0419$  and  $wR^2 = 0.0952$  for all (6957) intensity data. All hydrogen atoms could be found on the difference Fourier maps. Then the hydrogen atom positions were defined upon geometric evidences, and were refined by the riding model. The maximum and minimum peaks on the final difference Fourier map corresponded to 0.14 and -0.13 e.Å $^{-3}$ , respectively.

Crystallographic data (excluding structure factors) for the crystal structure of **1** (*S*) have been deposited with the Cambridge Crystallographic Data Centre as supplementary publication number CCDC xxxyyz.

### 2.3. Further analytical methods

FTIR spectra of the chiral and racemic compound (*S*)-**1** and (*R,S*)-**1** were measured by Excalibur Series FTS 3000 (Biorad) FTIR spectrophotometer in KBr between 400 and 4000 cm $^{-1}$ .

Powder X-ray diffraction patterns were recorded with an X'pert Pro MDP (PANalytical Bv., The Netherlands) X-ray diffractometer equipped with X'celerator

detector using Cu K<sub>α</sub> and Ni filter. In case of the highly crystalline (S)-**1** with well-grown crystals, a rotation of the sample stage with revolution time of 16s was applied in order to reduce to some extent the preferred orientation observed. For indexing of powder pattern of (R,S)-**1** and for space groups determination from a statistical assessment of systematic absences [<sup>13</sup>] the DASH structure solution package was used [<sup>14</sup>].

Differential scanning calorimetry (DSC) measurements were performed using a Modulated DSC 2920 apparatus (TA Instruments, US). The samples (1-3 mg) were measured in sealed Al-pans at a heating rate of 10 K/min. For temperature and enthalpy calibration of the DSC instrument pure In metal standard was applied.

Calculation of the eutectic composition, the eutectic temperature and the liquidus curves is based on combination of the simplified Schröder-van Laar (Eqs. 1 and 2) and Prigogine-Defay equations (Eq.3) [<sup>15,16</sup>]. Thus, liquidus curve ( $T^f$  melting temperature vs.  $x_S$  binary enantiomer composition) can be modeled in three stages (L<sub>1</sub>, L<sub>3</sub> and L<sub>2</sub>) over the whole composition range (0 ≤  $x_S$  ≤ 1):

$$\text{IF } L_1, \text{ ha } 0 \leq x_S \leq x_{eu}: \ln x_R = \ln(1 - x_S) = \frac{\Delta H_R}{R} \left( \frac{1}{T_R^f} - \frac{1}{T^f} \right) \quad (\text{Eq.1}),$$

$$\text{IF } L_2, \text{ ha } 1 \geq x_S \geq 1 - x_{eu}: \ln(x_S) = \frac{\Delta H_S}{R} \left( \frac{1}{T_S^f} - \frac{1}{T^f} \right) \quad (\text{Eq.2}),$$

$$\text{IF } L_3, \text{ ha } x_{eu} \leq x_S \leq 1 - x_{eu}: \ln[4x_S(1 - x_S)] = \frac{\Delta H_{RS}}{R} \left( \frac{1}{T_{RS}^f} - \frac{1}{T^f} \right) \quad (\text{Eq.3}),$$

where  $x_S$  and  $x_R$  (= 1 -  $x_S$ ) are molar fractions in the binary system of the enantiomers,  $T_S^f = T_R^f$ ,  $\Delta H_S = \Delta H_R$  are the melting points and molar enthalpies of fusion observed for the pure crystalline enantiomers, while  $T_{RS}^f$  and  $\Delta H_{RS}$  is the melting point and molar enthalpy of fusion of the racemate crystal, latter calculated for 1 mol R + 1 mol S composition.

### 3. Results and discussion

#### 3.1. Crystal structure of (*S*)-2-(2-nitro-1-phenylethyl)-1,3-diphenyl-propane-1,3-dione, (*S*)-1

(*S*)-2-(2-nitro-1-phenylethyl)-1,3-diphenyl-propane-1,3-dione, (*S*)-1 crystallizes in the orthorhombic crystal system, in the chiral space group  $P2_12_12_1$  (19) ( $Z = 8$ ,  $Z' = 2$ ). Detailed crystallographic data, the parameters of data collection, structure determination and refinement are presented in Table 1. There are two crystallographically independent molecules in the asymmetric unit (Fig. 1). They are chemically the same but different in conformation. The molecular overlay of the two crystallographically different molecules can be found in the crystal structure of (*S*)-1 is shown in Fig. 2a.

**Table 1: Summary of crystallographic data, data collections, structure determination and refinement for crystal (*S*)-1.**

Empirical formula	C <sub>23</sub> H <sub>19</sub> NO <sub>4</sub>
Formula weight (g/mol)	373.39
Temperature (K)	93(2) K
Wavelength	1.54187 Å
Crystal system, space group	Orthorhombic, $P2_12_12_1$
Unit cell dimensions	a = 10.6377(2) Å $\alpha = 90^\circ$ b = 11.4348(2) Å $\beta = 90^\circ$ c = 31.3543(6) Å $\gamma = 90^\circ$
Volume	3813.9(2) Å <sup>3</sup>
Z, Z', Calculated density	8, 2, 1.301 Mg/m <sup>3</sup>
Absorption coefficient	0.728 mm <sup>-1</sup>
F(000)	1568
Crystal size	0.77 x 0.42 x 0.41 mm
Theta range for data collection	6.85 to 71.74°
Limiting indices	-13 $\leq h \leq 11$ , -14 $\leq k \leq 12$ , -35 $\leq l \leq 37$
Reflections collected / unique	46848 / 6957 [R(int) = 0.0328]
Completeness to theta = 71.74	96.0 %
Absorption correction	Numerical
Max. and min. transmission	0.843 and 0.676
Refinement method	Full-matrix least-squares on F <sup>2</sup>
Data / restraints / parameters	6957 / 0 / 505
Goodness-of-fit on F <sup>2</sup>	1.131

Final R indices [ $I > 2\sigma(I)$ ]	$R_1 = 0.0377$ , $wR^2 = 0.0859$
R indices (all data)	$R_1 = 0.0419$ , $wR^2 = 0.0952$
Absolute structure parameter	-0.13(17)
Largest diff. peak and hole	0.227 and -0.199 e. $\text{\AA}^{-3}$

$$* w = 1/[\sigma^2(F_o^2) + (0.0222P)^2 + 1.1376P] \text{ where } P = (F_o^2 + 2F_c^2)/3$$

Figure 1. The molecules in the asymmetric unit of the crystal structure (*S*)-**1** and labeling of the atoms [17]. The displacement ellipsoids are drawn at the 50% probability level, heteroatoms are shaded. Ring assignations are indicated.

The structure of the 4-chlorophenyl derivative of **1** is known (CSD[18] refcode COQYEN) [2]. It crystallizes in the  $P2_1$  space group in the monoclinic crystal system. There are two molecules in the asymmetric unit also (Figure 2b). The conformation of molecules A and B in **1** is more similar than those of molecules A and B in the chloro derivative (Figure 2c).



**Figure 2** The molecular overlay [19] (N1-C5-C4 atoms are fitted) of the two molecules a.) in the asymmetric unit of (*S*)-**1** (molecule A is red, molecule B is blue), b.) in the asymmetric unit of COQYEN (molecule A is yellow, molecule B is green). c.) The molecular overlay (N1-C5-C4 atoms are fitted) of the four molecules either substituted or non-substituted by Cl.

There are four oxygen atoms in the molecule as anomalous dispersion centres only. The measurement was performed with Cu-K $\alpha$  radiation at low temperature -180°C. C4 atom in both crystallographically independent molecules has “S” configuration. The Flack x parameter is -0.13(17) [20].

Intramolecular C5-H5AA...O1 hydrogen bond contribute to the stability of both molecules in the asymmetric unit. An additional intramolecular interaction occurs in molecule “A” between the other hydrogen of C5 and the O3 oxygen. Because of the different conformation H5AB and O3 can be found on the opposite side of the molecule thus they are too far for an interaction in molecule “B”.

The unit cell contains no residual solvent accessible void. There is no classic hydrogen bond in the crystal structure. In spite there are potential acceptors in the molecule, in the absence of strong donors only weak C-H...O type interactions can be found in the crystal.

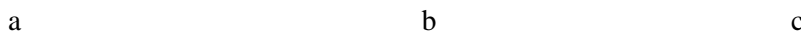


**Figure 3** The crystal packing of (*S*)-**1** [19]. a.) Molecular layer in the *ab* crystallographic plane composed of molecule A from the asymmetric unit. b.) Molecular layer in the *ab* crystallographic plane composed of molecule B from the asymmetric unit. c.) The alternating layers of molecule A (red) and B (blue) along the *c* crystallographic axis.

The two chemically identical but crystallographically different molecules construct two independent columns by weak C-H...O interactions (Figure 3) both are in the direction of the *b* crystallographic axis. These columns are repeated in the direction of the *a* crystallographic axis in an antiparallel manner in case of molecule A and parallel manner but shifted in case of molecule B. Additional week C-H...O hydrogen bonds occur among the molecules in case of molecule A in the *ab* crystallographic plane. C-H... $\pi$  weak interactions also support the stability of the molecular layers. The layers of molecule A and molecule B are alternating along the *c* crystallographic axis.

There are no strong  $\pi$ ... $\pi$  interactions in the crystal structure. The shortest ring distance in the crystal (Figure 4) is found between the rings containing C33 atom in molecules A and B. It is 4.073(1) $\text{\AA}$ , the rings are slightly shifted and their angle is 7.7(1) $\text{\AA}$ .

**Fig. 4** The week  $\pi\cdots\pi$  interaction between molecules A and B in the crystal structure of (S)-1 [19].

**3.2. Comparisons of (S)- and (RS)-2-(2-nitro-1-phenylethyl)-1,3-diphenyl-propane-1,3-dione, (S)-1 and (R,S)-1 by powder XRD and FTIR.**

The crystals of the chiral powder sample (**S-1**) have been very well-grown with relatively big crystallites, what caused that considerable and strongly variable preferred orientation could be observed without using a rotated sample stage. The effect of the preferred orientation still can be seen, if we compare the theoretically simulated powder pattern (Fig.5, profile on the top) generated from atomic coordinates of the single crystal

structure determination above, with the measured one (Fig.5, middle profile) applying a rotated sample stage during the diffraction measurement. Practically almost all reflections have occurred but with more or less different intensity ratios.

Fig.5. a) Simulated powder XRD pattern of (*S*)-**1** generated from the atomic coordinates of the single crystal structure determination (top); b) Experimental powder pattern of (*S*)-**1** measured on rotated sample stage in order to prevent preferential orientation (middle); c) Experimental powder pattern of racemic (*R,S*)-**1** with broad peak (with small crystallites)(bottom).

We can also recognize that the powder pattern of the racemic compound, (*R,S*)-**1** (Fig.5, bottom profile) significantly differs from those of enantiomeric (*S*)-**1**, i.e. the compounds have entirely different structures. The FWHMs (Full Width at Half Maxima) of peaks of (*S*)-**1** is significantly much smaller than those of (*R,S*)-**1**, indicating an excellent crystallinity (greater crystallite size) of (*S*)-**1**, compared to that of (*R,S*)-**1**.

Although, we could not increase the crystallinity of (*R,S*)-**1**, its diffraction pattern could be indexed to an orthorhombic unit cell [ $a = 22.18(7)$  Å,  $b = 17.08(3)$  Å,  $c=9.96(3)$  Å], and its most probable space group was determined to be *Pbca* (61) with  $Z = 8$  and  $Z' = 1$ . The latter value (number of formula units in one asymmetric unit) means, that both enantiomeric molecules in the crystal structure of racemic compound are actually in equivalent crystallographic positions, i.e. there is only one type of crystallographic environment of molecules in (*R,S*)-**1**.

The FTIR spectra of the chiral and racemic compounds (*S*)-**1** and (*R,S*)-**1** (Fig.6) are more or less similar, but present also differences arising from the crystallographically different *neighboring* secondary interactions of the vibrating molecules in each crystal lattice. Actually, there are two types of crystallographically independent and different molecular surroundings ( $Z'=2$ ) of crystal (*S*)-**1**, while there is only one and the same type of crystal force field of both enantiomeric molecules in lattice of (*R,S*)-**1**, where  $Z'=1$ .

Fig.6. FTIR spectrum of chiral (*S*)-**1** (top) and (*R,S*)-**1** (bottom) measured in KBr. Chiral crystals of (*S*)-**1** with two crystallographically independent molecules show more versatile  $\nu(\text{C=O})$  and  $\nu(\text{CH})$  vibration bands than (*R,S*)-**1** with crystallographically equivalent molecules.

The wavenumbers of the carbonyl C=O stretching vibration are seemingly sensitive to differences in the molecular interactions. In case of (*S*)-**1**, where the two crystallographically independent molecules involved in different number and strength of

C-H...O interactions (see above), three absorption bands (at 1692, 1671, 1656 cm<sup>-1</sup>) are observed, while in the racemic crystal (*R,S*)-**1**, where both mirrored enantiomer molecules take part in the same secondary interactions (as the symmetry transformations have no effect on the vibration frequencies and absorption coefficients), there are only two  $\nu(\text{C=O})$  stretchings at 1682 and 1655 cm<sup>-1</sup>, assignable to the two C=O bonds in the molecules. The CH stretching vibrations observed in the 2800-3100 cm<sup>-1</sup> range also exhibits increased number of absorption bands in case of (*S*)-**1** compared to those of (*R,S*)-**1**. Changes in wavenumbers and absorption probabilities have occurred in all the cases of the mentioned characteristic vibrations. C-C aromatic skeleton vibrations also effected by a shift of a wavenumber from 1558 to 1547 cm<sup>-1</sup> for the two compounds. The fingerprint region of various deformation vibrations also provide small variations in positions and intensity of absorption bands and peaks for (*S*)-**1** and (*R,S*)-**1**.

### 3.3. Differential Scanning Calorimetry (DSC) and compilation of binary melting phase diagrams for solid (*S*)-**1** and (*R,S*)-**1**.

The DSC measurements of pure crystalline (*S*)-**1** and (*R,S*)-**1** in sealed Al-pan show a melting point at 135.6 and 159.7°C and a corresponding enthalpy of fusion of 85.69 and 102.5 J/g, i.e. 32.00 kJ/mol for (*S*)-**1** and 76.55 kJ/mol for 1 mol *S* + 1 mol *R* formulae of (*R,S*)-**1**, respectively. The measured melting point of crystal (*S*)-**1** is significantly higher than the value of 127-128°C published for enantiomeric **1** [4].

DSC traces of some selected binary mixtures of enantiomeric and racemic compounds are shown in Fig. 7.

Fig. 7. DSC traces of two solid mixtures with enantiomeric excess (*ee.*) of 50% (top) and 82% (bottom). The occurrence of two peaks in the former case confirms the eutectic relation between the racemic and enantiomeric crystals. Meanwhile the composition of the latter mixture should be close to the eutectic composition, as only one melting peak has been observed at 133.9°C, at a bit higher temperature than the eutectic temperature 131.6°C detected above.

As expected, the enantiomeric and the racemic crystals behave as crystal mixture of conglomerates and exhibit a eutectic melting behavior. Estimation of the eutectic

molar fraction, eutectic temperature, and liquidus curves of binary eutectic phase diagrams have also been calculated numerically [21] based on the temperature and enthalpy of fusion of pure crystalline phases assuming the validity of simplified Schröder-van Laar equation in combination with the Prigogine-Defay equation [15, 16]. The calculated melting phase diagram of the binary (*R*)- and (*S*)-2-(2-nitro-1-phenylethyl)-1,3-diphenyl-propane-1,3-dione system, with racemic compound ((*R,S*)-**1**), is shown in Fig. 8. The calculated eutectic liquid composition in molar fraction is obtained as  $x_{eu,S}=0.064$ , while the corresponding eutectic temperature provided as  $T_{eu}=132.7^{\circ}\text{C}$ .

Fig.8. Calculated melting phase diagram of the binary (*R*)- and (*S*)- 2-(2-nitro-1-phenylethyl)-1,3-diphenyl-propane-1,3-dione system, with racemic compound ((*R,S*)-**1**) according to the simplified Schröder-van Laar equation in combination with the Prigogine-Defay equation.

## Conclusion

The structure of (*S*)-2-(2-nitro-1-phenylethyl)-1,3-diphenyl-propane-1,3-dione, (*S*)-**1**, (orthorhombic crystal system, space group  $P2_12_12_1$ , 19) has been determined by single crystal X-ray diffraction. There are two crystallographically independent molecules in the asymmetric unit. Powder XRD pattern of pure racemic compound (*R,S*)-**1** could be indexed to an orthorhombic unit cell, and its most probable space group was determined to be the centrosymmetric *Pbca* (61) with only one molecule in the asymmetric unit. The wider variety of secondary molecular interactions between the two crystallographically independent molecules present in the enantiomerically pure (*S*)-**1** has been reflected in the FTIR spectrum as increased number of  $\nu(\text{C=O})$  and  $\nu(\text{CH})$  vibration bands compared to those of racemic (*R,S*)-**1**. Based on the melting point and enthalpy of fusion measured by DSC for the pure (*S*)-**1** and (*R,S*)-**1** crystalline solids, the binary melting phase diagram in full range of the chiral and racemic compounds are successfully calculated.

From the calculation we obtained that the enantiomeric excess in the eutectic composition of **1** enantiomeric mixture is  $ee_{\text{Eu}} = 87\%$ . Consequently, the initial *ee* of the crude product ((*S*)-**1**, *ee* = 42%) was in the racemate side of the phase diagram and the racemic mixture

precipitated during crystallization, in accordance with the measured thermoanalytical data and calculations. However, precipitation of the racemate caused higher enrichment of the (*S*)-**1** enantiomer ( $ee = 94\%$  instead of  $ee_{Eu} = 87\%$ , Table 1, line 1) in the filtrate than it would be expected in thermodynamic equilibrium of crystallization. In other words, fast precipitation of (*R,S*)-**1** pushed the composition of the residual material in solution to the enantiomeric side of the phase diagram (instead of the eutectic composition) and the system could not achieve thermodynamic equilibrium before filtration. Jump of the eutectic composition (from the racemate side to the enantiomeric side) during the first crystallization was confirmed by the results of the second crystallization (Table 1, line 2) when purer enantiomeric mixture ( $ee = 96\%$ ) was obtained from the first crystallized fraction, than the initial ee (94%).

## Acknowledgements

V. Kudar and P. Bombicz acknowledge the support from the Hungarian Scientific Research Fund (OTKA K-100801).

## Legends for Figures

### Scheme 1. Regio and enantio selective synthesis of the title compounds

**Fig. 1.** The molecules in the asymmetric unit of the crystal structure (*S*)-**1** and labelling of the atoms [17]. The displacement ellipsoids are drawn at the 50% probability level, heteroatoms are shaded. Ring assignations are indicated.



**Fig. 2.** The molecular overlay [19] (N1-C5-C4 atoms are fitted) of the two molecules a.) in the asymmetric unit of (*S*)-**1** (molecule A is red, molecule B is blue), b.) in the asymmetric unit of COQYEN (molecule A is yellow, molecule B is green). c.) The molecular overlay (N1-C5-C4 atoms are fitted) of the four molecules either substituted or non-substituted by Cl.



**Fig. 3.** The crystal packing of (*S*)-**1** [19]. a.) Molecular layer in the ab crystallographic plane composed of molecule A from the asymmetric unit. b.) Molecular layer in the ab crystallographic plane composed of molecule B from the asymmetric unit. c.) The alternating layers of molecule A (red) and B (blue) along the c crystallographic axis.

**Fig. 4.** The week  $\pi\ldots\pi$  interaction between molecules A and B in the crystal structure of (*S*)-**1** [19].

**Fig. 5.** a) Simulated powder XRD pattern of (*S*)-**1** generated from the atomic coordinates of the single crystal structure determination (top); b) Experimental powder pattern of (*S*)-**1** measured on rotated sample stage in order to prevent preferential orientation (middle); c) Experimental powder pattern of racemic (*R,S*)-**1** with broad peak (with small crystallites)(bottom).

**Fig. 6.** FTIR spectrum of chiral (*S*)-**1** (top) and (*R,S*)-**1** (bottom) measured in KBr. Chiral crystals of (*S*)-**1** with two crystallographically independent molecules show more  $\nu(\text{C=O})$  and  $\nu(\text{CH})$  vibration bands than (*R,S*)-**1** with crystallographically equivalent molecules.

**Fig. 7** DSC traces of two solid mixtures with enantiomeric excess (ee.) of 50% (top) and 82% (bottom). The occurrence of two peaks in the former case confirms the eutectic relation between the racemic and enantiomeric crystals. Meanwhile the composition of the latter mixture should be close to the eutectic composition, as only one melting peak has been observed at 133.9°C, at a bit higher temperature than the eutectic temperature 131.6°C detected above.

**Fig. 8.** Calculated melting phase diagram of the binary (*R*)- and (*S*)-2-(2-nitro-1-phenylethyl)-1,3-diphenyl-propane-1,3-dione system, with racemic compound (*RS*) according to the simplified Schröder-van Laar equation in combination with the Prigogine-Defay equation.

## Legend for Tables

Table 1. Summary of crystallographic data, data collections, structure determination and refinement for crystal (*S*)-**1**.

## References

<sup>1</sup> C.-J. Wang, Z.-H. Zhang, X.-Q. Dong, X.-J. Wu, Chem. Commun. (2008) 1431-1433.

<sup>2</sup> B. Tan, X. Zhang, P. J. Chua, G. Zhong, Chem. Commun. (2009) 779-781.

<sup>3</sup> C. Min, X. Han, Z. Liao, X. Wu, H.-B. Zhou, C. Dong, Adv. Syn. Catal. 353 (2011) 2715-2720.

<sup>4</sup> D. P. Gavin, J. C. Stephens, ARKIVOC, 2011 (2011) (ix) 407-421.

<sup>5</sup> US Patent Application, US2012/004424(A1), Nanyang Technological University, 2012, (inventors: G. Zhong, B. Tan, X. Zhang, P. J. Chua).

<sup>6</sup> P. Kasaplar, P. Riente, C. Hartmann, M. A. Pericas, Adv. Syn. Catal., 354 (2012) 2905-2910.

<sup>7</sup> A. M. Flock, A. Krebs, C. Bolm, Synlett (2010) 1219 - 1222; Art.No: G05010ST.

<sup>8</sup> P. Kotrusz, S. Toma, H.-G. Schmalz, A. Adler, Eur. J. Org. Chem. (2004) 1577-1583.

- <sup>9</sup> Z.-B. Xie, N. Wang, M.-Y. Wu, T. He, X.-Q. Yu, Z.-G. Le, Beilstein J. Org. Chem., 8 (2012) 534-538.
- <sup>10</sup> CrystalClear SM 1.4.0 (Rigaku/MSC Inc., 2008).
- <sup>11</sup> NUMABS: Higashi, T. (1998), rev. 2002. (Rigaku/MSC Inc.).
- <sup>12</sup> G. M. Sheldrick, Acta Cryst., (2008) A64, 112-122.
- <sup>13</sup> A. J. Markvardsen, W. I. F. David, J. C. Johnson, K. Shankland, Acta Crystallogr., Sect. A 2001, 57, 47-54.
- <sup>14</sup> W. I. F. David, K. Shankland, J. Cole, S. Maginn, W. D. S. Motherwell, R. Taylor, DASH User manual; Cambridge Crystallographic Data Centre: Cambridge, U.K., 2001.
- <sup>15</sup> J. Jacques, A. Collet, S. H. Wilen, Enantiomers, racemates, and resolution, John Wiley & Sons, New York, 1981. pp. 47, 91.
- <sup>16</sup> Z. J. Li, M. T. Zell, E. J. Munson, D. J. W. Grant, J. Pharm. Sci. 1999, 88, 337-346.
- <sup>17</sup> A.L. Spek, Acta Cryst., (2009) D65, 148.
- <sup>18</sup> F.H. Allen, Acta Cryst. (2002) B58, 380-388.
- <sup>19</sup> C.F. Macrae, P.R. Edgington, P. McCabe, E. Pidcock, G.P. Shields, R. Taylor, M. Towler and J. van de Streek, J. Appl. Cryst., (2006), 39, 453.
- <sup>20</sup> H. D. Flack, Acta Crystallogr., Sect. A: Found. Crystallogr. 39 (1983) 876-881.
- <sup>21</sup> J. Madarász, D. Kozma, G. Pokol, M. Ács, E. Fogassy, J. Therm. Anal. Calorim. 42 (1994) 877-894.